SUMMARY OF ICE-MOTION MAPPING USING PASSIVE MICROWAVE DATA

J. Maslanik, T. Agnew, M. Drinkwater,W. Emery, C. Fowler, R. Kwok, A. Liu

November 1998

National Snow and Ice Data Center (NSIDC) Special Publication 8

Report prepared for NSIDC
at the request of the NSIDC Polar Data Advisory Group

1. Rationale

A number of investigators, including the co-authors of this report, are engaged in generating ice motion products from SSM/I imagery for a variety of applications. The Polar Data Advisory Group (PoDAG), concerned that unwarranted overlap might exist among these projects, has requested a summary of the different methods and results.

The objectives of this document are to:

- summarize the basic aspects of passive microwave- (SMMR- and SSM/I-) derived sea ice motion;
- provide an overview of several of the basic approaches currently being used to generate gridded ice-displacement information from SMMR and SSM/I data;
- summarize the overall accuracies expected from the different approaches;
- indicate some likely directions of future work.

Each approach discussed here uses different time intervals for calculating ice displacements, and applies differing degrees of data filtering and post-processing. This report therefore does not attempt a quantitative, one-to-one intercomparison of velocity vectors produced by the above investigators. Instead, we note the general similarities and differences among the methods and products. Examples of motion vectors for similar dates are provided for general comparison. This summary is limited to passive microwave investigations. However, a number of additional studies using buoys SAR, AVHRR, and scatterometer data are relevant to the issues of algorithms, accuracies, effects of temporal and spatial sampling, etc. We are aware that additional investigators other than those mentioned here are involved in efforts to generate ice products. To our knowledge, these other efforts use techniques basically similar to those discussed here.

2. Background

Within the last several years, sea ice researchers used animations of SSM/I 85 GHz data (e.g., T. Agnew and D. Cavalieri) or scatterometer imagery (M. Drinkwater) to illustrate that coherent motion of the sea ice pack could be seen in sequential relatively low-resolution microwave images. A number of investigators then began applying existing motion-detection methods developed for tracking ice motion in AVHRR and SAR data to SSM/I and NSCAT imagery.

Results show that the SSM/I- (and SMMR-) derived ice motions provide more frequent temporal sampling and a longer period of coverage (1979-present) than SAR, more consistent coverage than AVHRR, and more extensive spatial coverage than presently is provided by drifting buoys. The precision of the passive microwave-derived vectors,

however, is less than that achievable from these other data sources, and reliable motions cannot presently be calculated consistently during late spring through early autumn.

These initial efforts have been followed by additional research to refine the methods and to test alternative motion detection routines. The motion tracking routines used, and discussed here, include:

- Methods based on identifying maximum correlation between search areas in consecutive images. Individual, unique features are not followed over time;
- A wavelet method, which follows movement of particular wavelet-defined locations over time;
- Most methods apply some filtering to remove "erroneous" vectors;
- Some subjectivity comes into play in each method, through the selection of filtering criteria or choice of statistical parameters or processing options.

The key factors involved in deriving ice displacements from passive microwave data can be summarized as follows:

- Combinations of ice concentration and snow/ice emissivity variations within the sensors' field of view (approximately 14 km for SSM/I 85 GHz and 30 km for 18 and 19 GHz channels on SMMR and SSM/I [but mapped to grid cell sizes of 12.5 km and 25 km, respectively]) provide the identifying microwave "signature" that is tracked over time;
- Observed motions represent the ensemble displacement ("average motion") of this signature within the sensor's field of view, rather than the displacement of a point feature (such as that represented by buoy motions);
- Passive microwave-derived motions can be obtained at a higher temporal sampling rate than is the case for satellite SAR and better spatial coverage than existing buoys for most of the year;
- Spatial resolution of the existing data is the main factor limiting the precision of motion detection;
- Atmospheric conditions (cloud cover and columnar water content) and perhaps changes in surface condition due to melt are the main factors limiting the times of year when reliable motions can be observed;
- Rapid deformation and rotation within the pack, such as occurs in some MIZ regions, affects the regional accuracy of the motions;
- Other factors such as snowfall, ridging, etc. that can modify the microwave signature for a location might affect the ability to track individual ice parcels.

Some additional items common to the existing studies are:

- Drifting buoys (mainly the IABP buoys) have provided the bulk of the comparisons for accuracy assessments;
- Different approaches are used (e.g., interpolation or no interpolation, and different search-radius distances to buoys) when comparing buoy- and SSM/I-derived displacements;
- Basic error statistics among the different investigators' products are fairly similar and consistent;
- Accuracies relative to buoys are better than would be expected from a summation of the potential error terms;
- Variability in the microwave-derived motions in comparison to buoys is relatively high, but biases in the data are small on average. Errors and biases appear to vary by region. Some results suggest the errors are unbiased and Gaussian, which implies that errors are reduced substantially be averaging;

- Patterns of ice motion, even for daily displacements, appear consistent and realistic, but with some regional and seasonal variations;
- Atmospheric conditions and melt limit the useful period of passive microwave motions to approximately September - May for the Arctic;
- Weather effects tend to be more prevalent in the Antarctic;
- Ice displacements can be reliably detected from 37 GHz data as well as 85 GHz data, allowing production of motion fields for 1979-present using a combination of SMMR and SSM/I data.

Items that warrant specific note include:

- Little difference has been found to date between using horizontally- or vertically-polarized data, or between using channel combinations versus a single channel, although horizontal polarized data is mentioned (Agnew et al.) as visually showing more distinct features;
- Some differences between buoy displacements and satellite-derived displacements will always exist due to the nature of the two sampling methods (areally-averaged motion vs. point motion, etc., and different time sampling);
- Comparisons to SAR-derived motions are also affected by the difference in time sampling between the SAR- and SSM/I-observed displacements;
- The spatial distribution of buoys does not provide complete coverage of all areas, and thus error statistics relative to buoys will be more or less representative of the entire Arctic and Antarctic depending on the distribution (Figures 1 and 2 illustrate this);
- The uncertainty in the 37 GHz motions is less than would be expected given that the field of view is twice that of the 85 GHz channel;
- The relatively small bias in the microwave-derived motions implies that mean fields should be quite accurate, but the sources of error (atmosphere, ice deformation, etc.) are not necessarily independent of ice velocity and region, so could conceivably introduce biases into mean fields.
- The use of daily-averaged brightness temperatures (TBs) introduces some "smearing" of the motion pattern, which should affect the accuracy of the tracking. However, one study which examined use of non-averaged TBs found little difference compared to use of the averaged TBs;
- Comparisons among displacement vectors from buoys, SSM/I and 2-dimensional ice models suggest that the mean error statistics between the model and SSM/I are similar. Differences can be large though for individual time periods, and vary as a function of location, ice concentration, and ice thickness.

3. Summary of Investigators' Approaches and Results

3.1 T Agnew and collaborators

Agnew, T.A., H. Le, and T. Hirose, Estimation of large scale sea ice motion from SSM/I 85.5 GHz imagery, AES report.

Agnew, T.A., H. Le, and T. Hirose, Estimation of large scale sea ice motion from SSM/I 85.5 GHz imagery 1997, Annals of Glaciology, 25, 305-311.

Agnew, T.A., H. Le, and M. Shokr, 1998. Characteristics of large winter leads over the Arctic Basin from 85.5 GHz DMSP SSM/I and NOAA/AVHRR imagery. Can. J. Remote Sensing (in press).
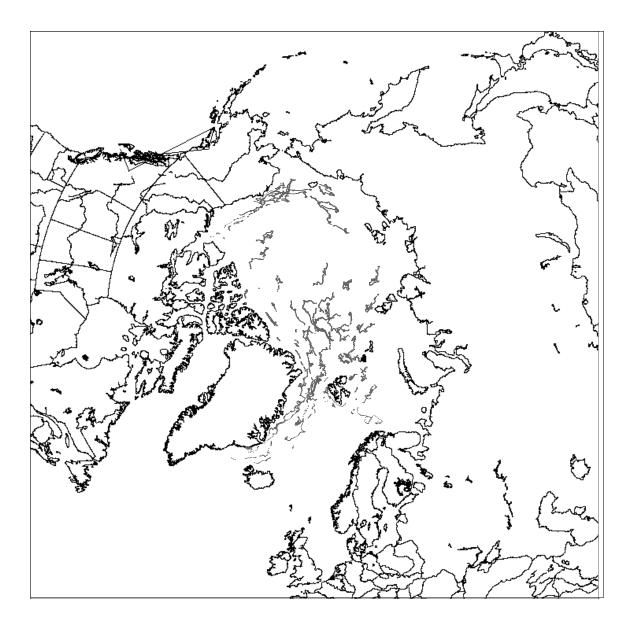
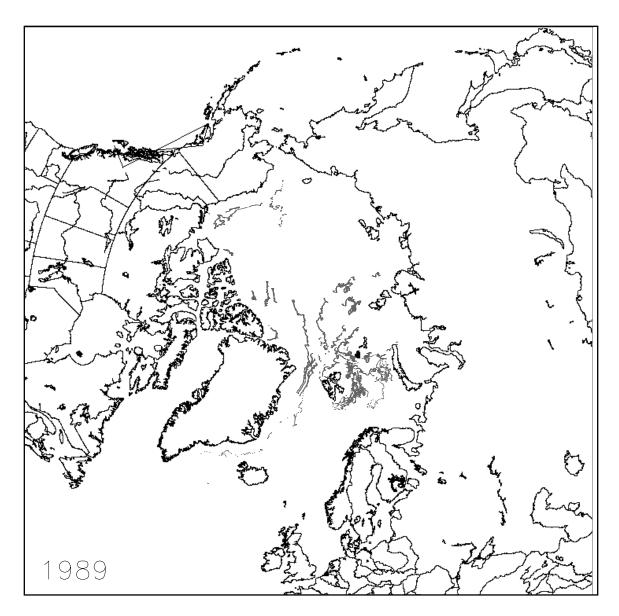Figure 1. Distribution of IABP buoys during 1988.

1989

Figure 2. Distribution of IABP buoys in 1989.

3.1.1 Basic features

- Applied to 85 GHz horizontally-polarized data. (NSIDC daily-averaged grids for the Arctic). A neighbor-substitution algorithm is used to fill in occasional missing pixels and scan lines;
- Uses a maximum cross correlation (MCC) method, with correlations calculated directly (e.g., without Fast Fourier Transforms [FFT]);.
- As applied here, the procedure is contained in a software package called Tracker (Hirose et al., 1991), and is completely automated.
- Displacements were calculated over different time intervals. Mostly displacements over 3 or 4 days.
- Cross-correlation search begins with the use of matching features ("seed locations") with sharp features as seen in full-resolution images. Based on seed locations, adjacent areas are searched using MCC applied to a search window. The search is guided by the

5

seed location displacement vectors and a knowledge of the maximum displacement that can be expected for ice motion.

- Estimation of ice displacement between images was done approximately every 6 pixels (75 km).
- A second pass through image may be done using a reduced correlation threshold to fill in unmatched areas.
- No filtering or removal of cloud was done. An error correction procedure was applied to check for consistency of displacement vectors with surrounding vectors.
- it is noted that motion within the search window must be representable as a single vector. An important advantage is that the resulting velocity fields possess a high degree of spatial continuity, which permits the calculation of spatial derivatives essential for investigating processes of ice deformation.
- IABP buoys were used for comparisons. Some "bad" buoy reports eliminated. Most of the buoys used for comparison were located in the western Arctic Basin.
- Three closest SSM/I estimates to the buoy locations are compared to buoy drift for same period. The three closest are interpolated for comparison to the associated buoy velocity.
- Comparison were done for periods in Nov., 1998, Dec. 1993 and Jan. 1994. These time periods were selected based on strong ice motion in the western part of the Arctic Basin and the relatively good Arctic buoy coverage.

An example of the ice displacements derived by T. Agnew and collaborators is shown in Figure 3. Note that the quality of many of the hard-copy figures included here is less than that of the originals. An on-line version of this document will be made available with high-quality figures as originally supplied by the co-authors.

3.1.2 Main findings

- Estimated theoretical error is 4.6 km/day (about 16.8 km divided by number of days over which displacement is calculated).
- Given average time separation between images of 3.6 days for the 25 runs, observed errors relative to buoys correspond to a vector magnitude error of 3.5 km/day (4 cm/s). Correlation coefficient for all comparisons = 0.75.
- The overestimate is perhaps due to a tendency for incorrect matches to occur for larger displacements than for smaller displacements.
- Error (uncertainty) in angle displacement is greater for slower motions than for faster ones.
- Comparisons show problems in tracking movement in the MIZ, particularly in north Greenland Sea;
- Results of case studies show ice motion consistent with atmospheric pressure patterns;
- Observed ice motion is used to illustrate processes involved in variations in leads and ice concentration;
- Preliminary results are mentioned that show use of individual swath data with radiometric correction and better geolocation does not significantly improve the comparison with buoys in the Arctic.
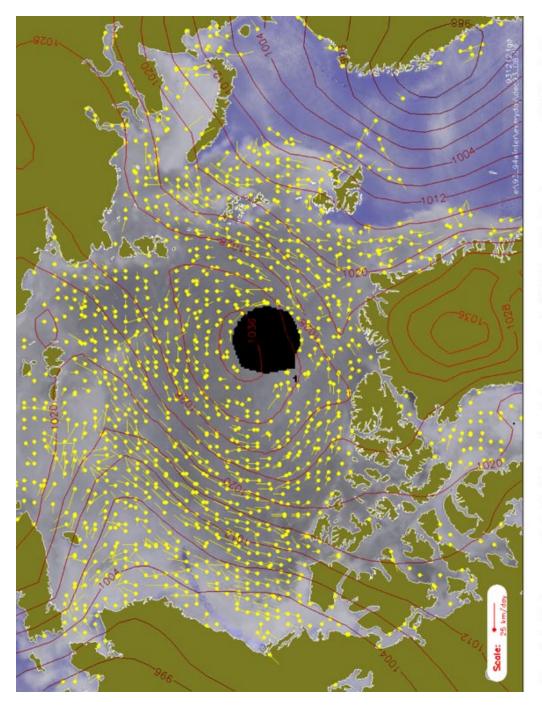
Figure 3. Ice Displacements calculated by T. Agnew for a displacement interval of 8-11 Dec. 1993. Also shown are mean NCEP sea level pressures for the same period.
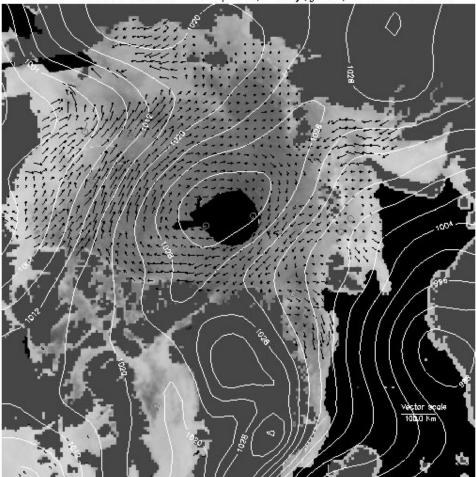
3.2 R. Kwok and collaborators

Kwok, R., A. Schweiger, D.A. Rothrock , S. Pang, and C. Kottmeier, 1998. Sea ice motion from satellite passive microwave imagery assess with ERS SAR and buoy motions. J. Geophy. Res., 103, C4, 8191-8214.

Kwok, R., J.C. Curlander, R. McConnell, and S. Pang, 19990. An ice motion tracking system at the Alaska SAR facility, IEEE J. Oceanic Engineering, 15(1), 44-54, 1990.

3.2.1 Basic features

- Comparisons are done for motions calculated using individual channels (37 GHz as well as 85 GHz data, horizontal and vertical polarizations) taken from daily-averaged grids with missing pixels replaced by median value of the 3 x 3 neighborhood;
- Cross-correlations are applied at two steps - first to original-resolution data, and then to oversampled data;
- This second step uses data oversampled by a factor of 6, which yields pixel spacing of 2.1 km for 85 GHz data and 4.2 km for 37 GHz data;
- Regions used for the correlation calculations are 100 km x 100 km for 85 GHz and 200 km x 200 km for 37 GHz;
- After each step, filters are used to discard outliers and inconsistent vectors;
- No interpolation is used to fill locations for which vectors were not found;
- A final step is applied to estimate sub-pixel displacements by fitting a bi-quadratic surface to the correlation values and then selecting the locating of the maximum of the function;
- FFT are used to improve computation speed;
- A final set of filters are applied. These include a check to eliminate locations that exhibit too-great a change in mean TB, and vectors that differ too much in drift direction from NCEP reanalysis wind velocities;
- The Arctic and Antarctic are partitioned into different regions, with motions calculated over different displacement intervals for the regions (3-day intervals in the Arctic Basin and 1-day intervals in Fram Strait, Baffin Bay and Weddell Sea);
- Kwok et al. (1998) present results for October 1992-May 1993 (Arctic) and March 1992-October 1992 (Antarctic);
- Comparisons are done to SAR-derived motions as well as buoys;
- Comparisons to buoys are done using grid points that are within 40 km of buoy or SAR motion vectors, and which are temporally closest.

Figures 4a-c show examples of ice displacements calculated by R. Kwok. Figure 4a includes approximately the same time period as is shown in Figures 3 and 6. Figure 4b covers the same period as in Figure 7.

Figure 4a. 3-day displacements for 8-10 Dec. 1993 as calculated by R. Kwok. Also shown are NCEP mean sea level pressures for the same period. Buoy locations and displacements are shown in white.
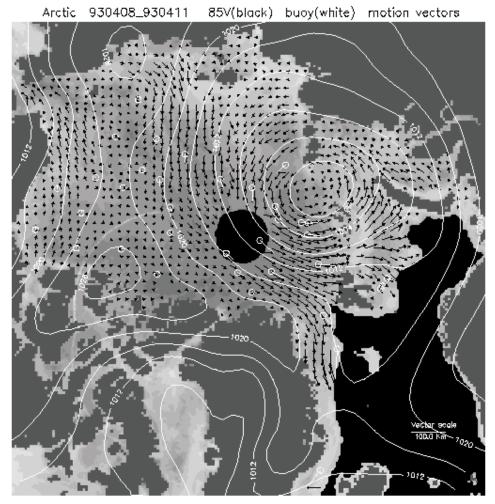
Figure 4b. 3-day displacements for 8-11 April 1993 as calculated by R. Kwok. Also shown are NCEP mean sea level pressures for the same period. Buoy locations and displacements are shown in white.

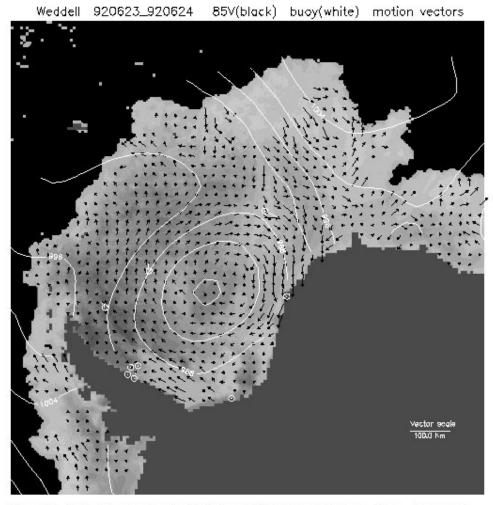Weddell 920623_920624 85V(black) buoy(white) motion vectors

Figure 4c. 1-day displacements for 23-24June 1992 as calculated by R. Kwok. Also shown are NCEP mean sea level pressures for the same period. Buoy locations and displacements are shown in white.

3.2.2 Main findings

- Summer ice motions become problematic due to atmospheric conditions and changes in the surface. Data thus become unreliable between melt onset and freeze-up;
- It is noted that the method of creating SSM/I daily-averaged TBs will cause a distortion in features. The degree of distortion is a function of drift speed.   Decorrelation of the buoy and SSM/I observations is expected if large local velocity gradients exist.
- It is noted that errors in motion estimates are dependent on the tracking and filtering process. Thus, some filters, which may effectively remove outliers, could inadvertently introduce biases.
- Standard deviations of the error range between 5 and 12 km, or about 4.2 cm/s using 3-day displacements in the Arctic Basin, 6.1 cm/s using 1-day displacements in Fram Strait, 6.9 cm/s in the Weddell Sea;
- Correlations range between 0.76 for the Arctic Basin and Fram Strait to 0.67 for the Weddell Sea;
- Comparisons to buoys warrant some examination of the individual buoys themselves. Some larger errors appear in Weddell Sea due to some buoys near the coast being motionless at times;
- Excluding small motions from comparisons has a large effect on statistics, but it is not recommended that small motions be excluded from the data set, since these errors will be averaged out when means are calculated over longer time periods. For example, error standard deviation in the 3-day Arctic Basin displacements reduces from 4.2 cm/s to about 2.3 cm/s, and to about 4.5 cm/s for 1-day displacements in Fram Strait. Correlations also improve substantially;
- Uncertainty in 37 GHz results are only slightly worse than is case for 85 GHz.
- Comparison with SAR suggests that SSM/I correlates better with SAR, probably because SAR, like SSM/I, provides a spatially-averaged motion. Average correlations are higher and directional differences are lower than with the buoy comparison. Uncertainty and biases are, however, similar to the buoy comparison.
- Bias error appears to be due to error in the direction parallel with the motion, rather than in the perpendicular direction. Mean error seems to be biased by a small number of SSM/I observations that underestimate ice motion;
- Larger errors relative to buoys appear to occur where ice concentration is less. It is also possible that buoy motions in these areas are less representative than is the "average" motion provided by SSM/I.
- Larger errors occur in conjunction with large displacements. This population of errors introduces a small bias in the mean;
- Motion fields are consistent with atmospheric pressure patterns and winds as seen in comparisons of bi-monthly data;
- Comparisons are provided among mean SSM/I motion fields and motion fields generated from interpolated buoy positions and winds. Some notable differences are apparent. Also, the greater coverage of the SSM/I data compared, particularly in the Siberian coastal waters and the Kara Sea, is illustrated.

3.3. A. Liu and collaborators

Liu, A.K. and D.J. Cavalieri, 1998. On sea ice drift from the wavelet analysis of the Defense Meteorological Satellite Program (DMSP) Special Sensor Microwave Imager (SSM/I) data. Int. J. Remote Sensing, vol. 19, no. 7, 1415-1423.

Liu, A.K. and Y. Zhao, 1998. Sea ice motion from wavelet analysis of satellite data. Proc. 8th. International Offshore and Polar Engineering Conf., Montreal, Canada, May 24-29, 1998, 30-35.

Liu, A.K., Y. Zhao, and W.T. Liu, 1998. Sea-ice motion derived from satellite agrees with buoy observations. Eos Trans., AGU, vol. 79, no. 30, 353, 359.

3.3.1 Main features

- Uses a wavelet approach, based on SAR-application results that suggest ability to track motion under conditions that limit other methods.
- Uses 2-day displacements. The wavelet transform applied with a scale of 2 units of pixel spacing (25 km). The resulting contour is framed in a rectangular window. Each window at a given starting date is used as a template to be matched. The template window is not fixed in size, but is determined by the ice feature at a particular location.
- The domain of the template-matching between days can be restricted based on the maximum expected ice displacement. Two tracking regions are considered: coast/bay for fast ice motion (with a two-day sliding window), and central Arctic for slow ice motion (with a four-day sliding window). Template matching is performed with the results from the wavelet transform of the images between day 1 and day 5 for the central Arctic and between day 2 and day 4 for coast/bay areas. Template match is done by shifting the template over each pixel in the domain. Summation of the absolute value of the differences between the shifted template values and the target values is computed at each location. The sequence of the summation values is used a metric of the degree of match of the ice feature. Once the shapes have been matched, the velocity vector is estimated by dividing the relative displacement over the time interval. The method is described as being efficient because the only computations involved are logical operations (addition and subtraction).
- A two-day displacement interval is used for some examples. Five-day displacements are used for other examples.
- Using this approach, individual features are tracked for as long as possible, then a new feature is selected;
- Vectors are averaged to a 100 km x 100 km grid with outliers filtered;
- The method is applied to scatterometer data as well as SSM/I, for Arctic and Antarctic.
- Examples are provided for December 1992 through January 1993, December 1996, February 1997 for Arctic and June-July 1992;
- Used displacements within 8 km of buoy locations for general statistical comparisons;
- Comparisons include time series plots of SSM/I-derived displacements compared to an individual buoys for a 40-day period in winter 1993 and during December 1996, using features within a few pixels of the buoy;
- Comparison statistics are based on data mostly in the central and western Arctic;
- The method has also been applied to the Antarctic. Examples are presented for 29 June 1992 and 21 July 1992. No buoy comparisons given.

Figure 5 (taken from Liu and Zhao, 1998) illustrates motion vectors calculated by Liu and others for 22 Feb. 1997 using SSM/I and NSCAT data.
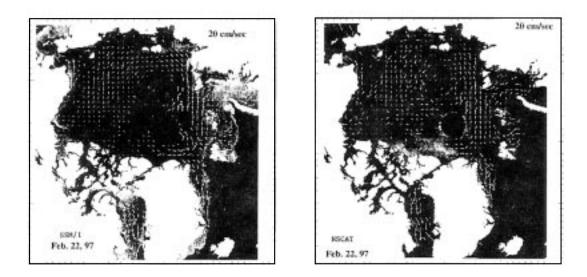
Figure 5. Comparison of SSM/I and NSCAT vectors. From Liu and Zhao (1998).

3.3.2 Main results

- Wavelet analysis is more interactive and is a research tool at this stage since one needs some knowledge of physical scales of ice features involved for the wavelet transform. Since the wavelet transform is based on FFTs, it is very efficient computationally and needs about 10 minutes for a motion map using a workstation. Therefore, wavelet analysis is definitely complementary to the correlation method and can make a major contribution to the understanding of ice drift over large areas at relatively high temporal resolutions.
- Derived drift patterns for two Antarctic examples are discussed, and are consistent with expected circulation;
- Comparisons to For 27 buoys (12 Dec.) yields standard deviation of 2.6 cm/s. For 12 Jan. (24 buoys), stand. deviation = 2.9 cm/s;
- For a 40-day period in 1993, motions are compared to an individual buoy in the Beaufort Sea. Speed and direction of the ice feature are tracked from the displacement between the two minima of the wavelet transform results nearest to the buoy. Speed difference for the 40-day period between the wavelet feature and buoy yields a std. deviation of 4.3 cm/s;
- The comparison of NSCAT and SSM/I derived ice motion with the Arctic Ocean buoy data (4-days sliding window) shows good overall agreement as indicated by the RMS values of differences in speed (2.8 cm/s and 3.0 cm/s). These values are also consistent with the estimate of satellite data uncertainty. For example, a feature displaced 25 km (NSCAT resolution) over 4 days will have a computed speed of 6.25 km/day (7.2 cm/s). In this case, for a template matching, the uncertainty in the estimate is 3.6 cm/s. Therefore, 4-day sliding window is required in central Arctic for the estimate of sea ice velocity. Using daily map, the temporal uncertainty of exact starting and ending time for a 4-day sliding window is approximately 1 day which is 25% of sea-ice drift. Therefore, a shorter time sliding window has larger uncertainty on sea-ice drift estimate (e.g., 2-day sliding window may have 50% error for sea ice drift);
- Analyses of 5-day displacement fields for Dec. 1992 suggest that major circulation patterns change significantly within 4- to 7-day periods. Daily motion fields are needed for data assimilation. Displacements over longer intervals could result in underestimates of open water production;

14

- Liu and Cavalieri (1998) used a single wavelet scale, while Liu and Zhao (1998) used multiple wavelet scales. The latter yielded a larger number of vectors.

3.4 C. Fowler and collaborators

Emery, W.J., C.W. Fowler and J.A. Maslanik, 1997. Satellite-derived maps of Arctic and Antarctic sea ice motions: 1988-1994. Geophys. Res. Lett., 24, 897-900.

Emery, W., C. Fowler and J. Maslanik, 1997. New satellite derived sea ice motion tracks Arctic contamination. Marine Pollution Bulletin, vol. 35, Nos. 7-12, 345-352.

Maslanik, J.A., C. Fowler, J. Key, T. Scambos, T. Hutchinson, and W. Emery, AVHRR-based Polar Pathfinder products for modeling applications, Ann. Glaciol., 25, 388-392,1998.

3.4.1 Main features

- Two versions of passive microwave-derived motions have been examined. Version 0 used a maximum cross-correlation method with oversampling by factor of 6; Version 1 uses MCC with a relaxation method which chooses most-likely displacement based on consistency with neighboring vectors;
- NSIDC daily-averaged TBs are used, with missing pixels filled by neighborhood averaging;
- Displacements calculated over 1-day intervals for all locations, with daily displacements also averaged over longer time periods into monthly and annual means;
- Vectors are mapped to a 62.5 km grid;
- Version 0 vectors filtered based on deviation from velocities in neighborhood;
- Version 1 vectors have no post-processing filtering applied, but with spatial-consistency filtering done during the relaxation process;
- Version 0 daily displacements have been calculated from 85 GHz and 37 GHz, for 1979 -1987 (SMMR) and 1987-1997 (SSM/I) for the Arctic and Antarctic;
- Version 1 daily displacements are currently available for 1988-1989 and 1993 for the Arctic;
- Version 0 SMMR and SSM/I motions have been used to validate ice model and climate model simulations and to calculate ice-transport trajectories;
- Version 0 SSM/I motions have been compared to buoys and model-derived motions as function of year, season, region and ice conditions;
- Some comparisons also done for the Antarctic;

Figures 6 and 7 show multi-day averages of daily displacements calculated by C. Fowler. The times of coverage correspond to Figure 3 and Figures 4a and 4b.
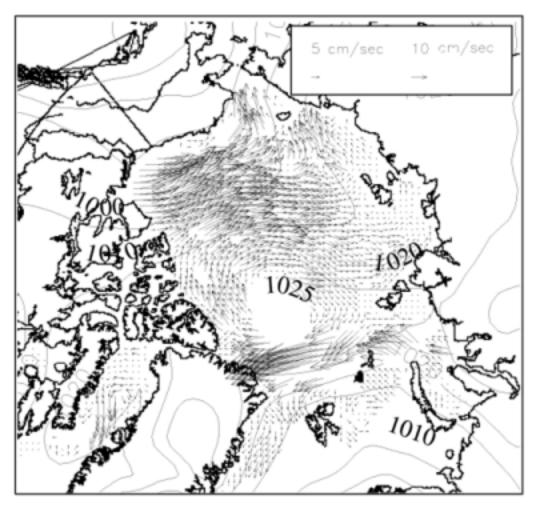
Figure 6. Mean ice displacements calculated from 24-hour displacements for 7-11 Dec. 1993. Mean NCEP sea level pressures are also shown. Vectors are "CCAR Polar Pathfinder Version 1" data.
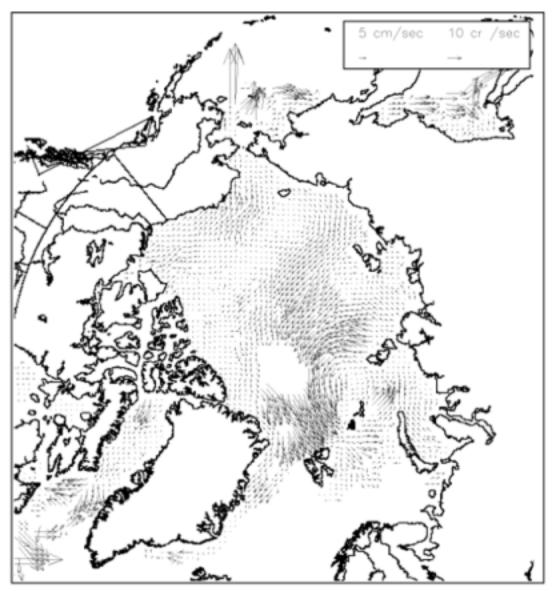
Figure 7. Mean displacements for 8-11 April 1993, averaged from daily CCAR Polar Pathfinder Version1 displacements. Note the erroneous vectors in Bering Strait that would require post-processing filtering to remove.

3.4.2 Main results

- Motion fields (daily fields as well as monthly, seasonal, and annual averages) are consistent with atmospheric circulation;
- Antarctic mean motion fields illustrate details of climatological circulation features;
- The 1-day displacements, monthly means, and climatologies have been used to evaluate ice models and GCM output;
- The Version 0 vectors show regional and seasonal differences in accuracy compared to buoys, with some dependence on ice conditions;
- Statistical comparisons with buoys vary somewhat from year to year for 1988-1993, probably due to the different regional distribution of buoys in different years (see Figures 1 and 2).   SSM/I vectors agreed best with the buoys during the year with the most uniform and extensive buoy coverage (1993);
- For 1988-1993, September - May, error standard deviation is about 5.5 cm/s for all Arctic motions (1-day displacements) using Version 0 vectors interpolated (a localized Cressman weighted interpolation) to the ice model grid. A total of 21,631 comparison pairs used for statistics;
- Error std. deviation for the Version 0 motions ranges from a maximum of 6.4 cm/s in 1988 to a minimum of about 4.8 cm/s in 1993. Correlations average about 0.65, with maximum of about 0.76 in 1993. Bias is less than 1 cm/s.
- Comparisons done using 85 and 37 GHz motions for 1992. Std. deviation error for 85 GHz is about 5 cm/s versus 7 cm/s for 37 GHz motions;
- Std. deviation of error (Version 0) for individual regions ranges from minimum of 5.1 cm/s in Siberian coastal waters to maximum of about 6.9 cm/s in Fram Strait;
- Partitioning of errors in Fram Strait shows substantial underestimation of drift speed by SSM/I, with errors particularly large for grid cells near the Greenland coast;
- For the Antarctic, the SSM/I Version 0 vectors have been used to calculate derivative fields of ice motion using 1-day displacements and 1-day displacements averaged over 3-day and 6-day intervals and for monthly mean motion fields. RMS error compared to buoys is about 7.7 cm/s using 1-day displacements, 4.7 cm/s using a 6-day average of 1-day displacements;
- Errors for the 85 GHz Version 1 vectors (24-hour displacements generated using a MCC with relaxation and with no interpolation; compared to buoys within 50 km) have been calculated for Jan. - 15 March 1988 for the Arctic. Mean error and RMS error are 0.6 and 6.5 cm/s (u component) and -0.7 and 6.8 cm/s (v component). Restricting the comparison to buoy velocities of 10 cm/s yields mean error and RMS error of 0.3 cm/s and 3.3 cm/s (x component) and -0.4 cm/s and 3.9 cm/s (y component). RMS error for all drift speeds but excluding Fram Strait yields RMS error of 5.0 cm/s (x component) and 4.9 cm/s (y component).

3.5 Drinkwater and Collaborators

Long, D.G., and M.R. Drinkwater, Cryosphere Applications of NSCAT Data, *IEEE Trans. Geosci. and Remote Sens.*, In Press.

Drinkwater, M.R., Satellite Microwave Radar Observations of Antarctic Sea Ice. In C. Tsatsoulis and R. Kwok (Eds.), *Analysis of SAR Data of the Polar Oceans*, Chapt. 8, 147-187, Springer-Verlag, Berlin, 1998a.

Drinkwater, M.R., Active Microwave Remote Sensing Observations of Weddell Sea Ice. In M.O. Jeffries (Ed.) Antarctic Sea Ice: Physical Processes, Interactions and Variability,

Antarctic Research Series., 74, 187-212, American Geophysical Union, Washington, D.C., 1998b.

Drinkwater, M.R., Satellite Microwave Radar Observations of Climate-Related Sea-Ice Anomalies, *Bull. Am. Met. Soc*., Proc. Workshop on Polar Processes in Global Climate, 13-15 Nov., 1996, pp. 115-118, 1997.

Drinkwater, M.R., and X. Liu, Satellite Observations of Southern Ocean Sea-Ice Circulation and Dynamics (OS51B-4), Western Pacific Geophysics Meeting, Taipei, Taiwan 21-24 July, 1998 Eos Transactions, American Geophysical Union, Vol. 79, No. 24, p46, June 16, 1998.

Drinkwater, M.R. and X. Liu, ERS Satellite Microwave Radar Observations of Antarctic Sea-Ice Dynamics, *Proc. 3rd ERS Scientific Symposium*, 17-20 March, 1997, Florence, Italy, ESA Publications Div., SP-414, ESTEC, Noordwijk, The Netherlands, 1109-1114, 1997.

Drinkwater, M.R. and X. Liu, Observing Interannual Variability in Sea-Ice Dynamics using NSCAT, Proceedings of NSCAT Science Team Workshop, Honolulu, Hawaii, 23-24 Jan., 1997, *JPL Tech. Pub*. , Jet Propulsion Laboratory, 4800 Oak Grove Drive, Pasadena, CA 91109, 1997.

3.5.1 Basic Features

- Techniques developed for tracking and gridding low-resolution radar and radiometer ice motion data (MCC methods described above) were employed by Drinkwater and collaborators. ERS and NSCAT Scatterometer and SSM/I motion products analyzed include (a) one-day gridded SSM/I-tracked motion, and (b) 6-day averages of smoothed SSM/I 1-day motion (for compatibility with the Scatterometer products).
- ERS and NSCAT ice motion data were computed at 3-day intervals.   Scatterometer image data tracked in conjunction with R. Kwok using the method described in Section 3.2 above. For ERS-1 Scatterometer images, the effective resolution for a stationary target is ~20-25 km, and the gridded pixel spacing 8.9 km (i.e. that imposed by the fine-resolution gridding in the imaging algorithm). In contrast, the NSCAT effective resolution is 8-10 km, and the pixel spacing 4.45 km. Effective resolution in the scatterometer images depends on latitude, sampling considerations and measurement overlap. Vectors were regridded at 10 pixel spacing (where pixel spacing in ERS Scatterometer products is ~ 8.8 km) Gridded vectors at 88 km intervals.
- ERS-1 data were oversampled by a factor of 4, which yielded a pixel spacing of approximately 2.2 km (consistent with sampling used for 85 GHz SSM/I data).
- Antarctic SSM/I data were tracked by C. Fowler (Section 3.4 above) and then analyzed in conjunction with buoy validation data supplied by the World Climate Research Program International Antarctic Buoy Program (WCRP-IPAB) participants;
- Comparisons with buoy data were made using gridded vectors within 50 km of the buoy measurement ;
- Products were compared on a similar polar stereographic grid projection with the x axis oriented at 90°E and the y axis parallel to the 0° meridian, to facilitate overlaying the vector products onto the radar scatterometer images from ERS-1/2 and NSCAT, together with NSIDC passive microwave images, and SAR data from ERS-1/2 and Radarsat;
- Consistent gridded ice motion data sets have been generated from each data source (at 3 and 1 day intervals, respectively) for an entire year in 1992.

Figures 8 and 9 illustrate SSM/I- and NSCAT-derived ice displacements for the Antarctic.
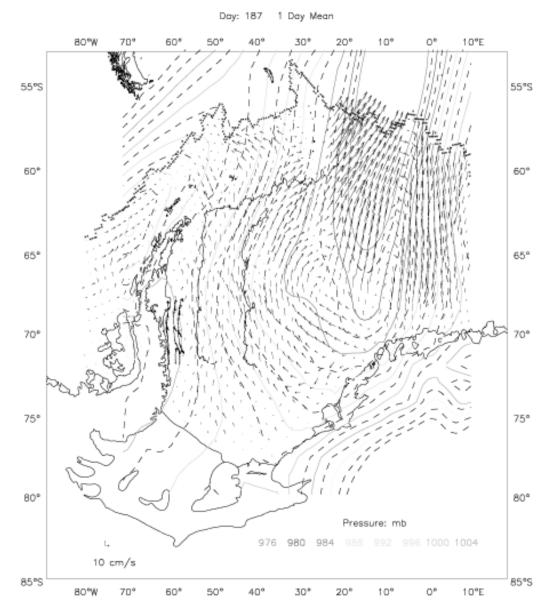
Figure 8. Weddell Sea 24-hour SSM/I ice motion and ECMWF surface air pressure field for day 187, 1992 (July 5). Buoy vectors are highlighted in red.
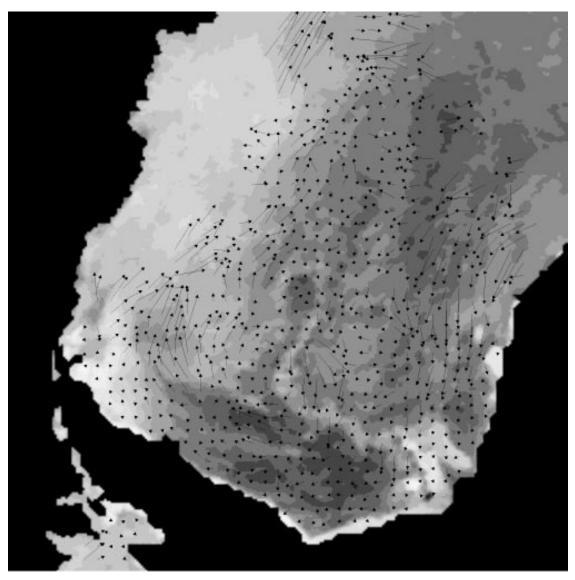
Figure 9. NSCAT v-pol image from day 273 (29 Sept.) 1996, superimposed by ice motion vectors for the 3-day period between day 273 and 276 (1 Oct. 1996).

3.5.2 *Main Results*

ERS-1 Scatterometer Data:

- Results show that the Scatterometer-derived motions are aliased, due to the irregular sampling intervals over the 6-day temporal averaging period. The result is a relatively poor comparison with Weddell Sea buoy-derived drift.
- 3-day RMS tracking errors were computed relative to the buoy reference displacement vectors in the Weddell Sea, Antarctica, where $error_{x,y} = buoy_{x,y} - vector_{x,y}$. The resulting rms errors are;

  3 day x displacement error = 2.36 pixels = 21.0 km - or of the order of 9.56 over-sampled pixels (spaced at 2.2 km intervals). This is the equivalent of a 7.0 km/d (8.1 cm/s) velocity error.

3-day y displacement error = 2.27 pixels = 20.2 km - or of the order of 9.2 over-sampled pixels. This is the equivalent to a 6.73 km/d (7.79 cm/s) velocity error.

Combined 1 day displacement and velocity errors for ERS-1 Scatterometer are 9.7 km/d and 11.22 cm/s, respectively.

- Errors in the Weddell Sea indicate that buoys on the shelf respond significantly to tidal currents, and aliasing of the tidal component is an important consideration. Comparisons with 1-day SAR drift confirms the small-scale response to semi-diurnal and diurnal tidal components. The greater high frequency variance in the buoy component of the tidal currents appears to contribute significantly to the underestimation of the motion by the scatterometer. The scatterometer tends to sample the underlying weekly mean ice drift, due to mean synoptic conditions.
- Drinkwater has presented mainly climatological ERS Scatterometer results due to the deficiencies of the 1-day SSM/I products, and the relative inaccuracy.

Weddell Sea SSM/I Motion Data:

- Comparisons of the CCAR-tracked (Version 0 vectors, as described in Section 3.4) Antarctic SSM/I datawith the buoy drift data (computed in a similar manner to that described above) indicate errors as follows;

The 1-day RMS errors for x and y component displacements were similar at 0.76 pixels (6.7 km) and 0.79 pixels (7.0 km), respectively.. Thus the 1-day RMS vector displacement and speed errors are approximately 9.7 km/d and 11.23 cm/s, respectively. Clearly the RMS pixel error is less than the scale of 1 original SSM/I pixel. However, as Kwok et al. (1998) have pointed out, the daily ice motion estimates are very noisy.

- 6-Day average of 1-day motions were investigated since they are most comparable to the tracking products derived using scatterometer images. As expected the result indicates that the rms errors decrease approximately in proportion to $1/\sqrt{n}$. The errors for the 6-day mean motion fields are as follows;

The x and y rms errors are reduced to 4.1 km (4.7 cm/s) and 4.18 km (4.8 cm/s) respectively. This is a significant improvement in the 1-day fields, and suggests that the creation of climatologies is a far more suitable solution than offering daily motion fields at the present time.

Seasonally-varying Autocorrelation Function:

- The CCAR daily SSM/I velocity statistics (Section 3.4; Version 0 vectors) have been used to investigate the seasonally varying form of the autocorrelation function. The gridded vectors were used to compute lagged correlations in the x and y projection directions for the polar stereographic projection u and v velocity components. An exponential fit to the results provided a method of evaluating the e-folding length scales (L_x, L_y), which are summarized in the table below;

U	Jan-Mar	Apr-Jun	Jul-Sep	Oct-Dec
Lx(km)	252.221	319.803	354.097	564.447
Ly(km)	301.431	537.865	755.1	856.935
V				
Lx(km)	291.357	383.813	740.111	717.509
Ly(km)	218.158	401.315	505.778	714.488

- The e-folding length scale is both anisotropic and seasonally dependent. Plots created prior to averaging in the x and y directions also indicate regional dependencies in the length scales, due to the fact that Antarctic sea ice does not simply comprise an annulus. Motion within the two primary Gyre circulations (i.e. in the Weddell and Ross Seas) have different length scales.

4. Summary of Comparisons

As described above, performance of the motion retrievals has been considered through quantitative comparisons with drifting buoys and to a lesser degree with SAR, NSCAT, and modeled motions, and qualitatively through comparisons to sea level pressure fields, winds and ice model output. All investigators find good agreement with sea level pressure (SLP) fields, using primarily NCEP and ECMWF reanalyses. Discrepancies can be found in some comparisons of individual days, which may indicate errors in the pressure fields. Typically, additional details of the ice motion can be seen in the microwave-derived fields than can be inferred from the lower-resolution SLP data. The SSM/I-derived velocity grids cover areas where consistent buoy data are not available. Such areas without buoy coverage include the Kara Sea, Hudson Bay, Baffin Bay, Bering Sea and Sea of Okhotsk, as well as much of the Southern Ocean.

On average, bias in the ice motion derived from 85 GHz data appears to be small, although errors in displacement estimates in Fram Strait contribute substantially to the mean bias. The standard deviation of the error (difference between buoy and SSM/I displacements) ranges from about 3 cm/s using 4-day displacements to about 5 to 6 cm/s using 1-day displacements. Correlations are about 0.7 - 0.8. Errors are greater for 37 GHz-derived motions, but the increase in error versus 85 GHz is less than might be expected given that the data resolution is about half that at 85 GHz. Some regional and seasonal variations appear in the error statistics, as well as variations related to ice concentration. Since the distribution of buoys is not random, varies from year to year, and does not cover all areas sampled by the SSM/I motions, at least some of the variations in statistics may be related to the available sample of buoys.

5. Conclusions

All of the approaches discussed here serve to demonstrate the feasibility and utility of deriving ice motion from passive microwave data. Three of the groups use variants of the cross-correlation technique, with the fourth group using wavelet analysis. The cross-correlation methods differ mainly in the degree of oversampling used, the approaches for filtering ice vectors to remove outliers, and the time interval between images used for the displacement calculations. Error statistics compared to buoys are similar among all the studies. Qualitative comparisons of examples from each group suggests that each method generates a similar number of SSM/I-derived vectors. Retrieval of vectors during late spring through late summer remains a problem, but the wavelet approach, and perhaps improved filtering methods for MCC-derived vectors, may provide some useful data during this period. The utility of the 37 GHz data allow motions to be estimated for 1979-present. Ice transport patterns consistent with winds can be seen in motions sampled on intervals as fine as 24 hours, but the noise level of daily displacements is high. Reduction of the nearly Gaussian noise through time averaging is effective at producing useful mean fields and climatologies.

5.1 Future Work

Data volume is small enough, and algorithms are fast enough, to permit generation of multiple years of motion vectors with a fairly small computation effort. In terms of continued work on methods, most of the comparisons to date have emphasized the Arctic. Additional work is needed to further assess performance in the Antarctic. Additional summations of accuracies as a function of region, season, and ice conditions will help guide potential uses of the data, and are needed for data assimilation efforts. Methods will continue to be refined, and combinations of methods to overcome limitations and to improve retrievals during marginal conditions is possible. More work is likely to be warranted to document whether orbital data, rather than the 24-hour averaged TBs used by each group, offers significant improvements. Such improvements might be expected for locations where ice velocities and rotation are large (such as Fram Strait and marginal ice zones) and/or when variable atmospheric conditions or melt cause decorrelation of TB patterns from one day to the next.

It can be expected that emphasis will shift from algorithm development and testing to address areas such as methods of merging or blending vectors from different data types (buoys, SAR, scatterometer, and AVHRR), and to applications of the ice motion data. Each group is investigating different methods or various aspects of the issues involved in combining data sets. Optimal interpolation of SSM/I velocities to fill in gaps in the data and to merge the SSM/I displacements with buoy observations has been performed by several of the investigators. However, the best procedure to use, and the necessary information to achieve best results, remains to be determined. For example, M. Drinkwater has calculated correlation length scales, which are needed for optimal interpolation of Antarctic data sets. He finds that further analyses of regional dependencies must be investigated to find a solution for generating seamless Southern Ocean wide gridded products, without having to regionally compartmentalize the data for optimal interpolation. C. Fowler found this to be the case when generating a multi-year time series of interpolated 85 GHz vectors for the Antarctic. In this case, interpolation introduced errors in the Palmer Peninsula area, and the strong gyre motion in the Antarctic limited the accuracy of assumptions of isotropy in the correlation field. H. Liu et al. (1998) suggest the use of data assimilation as a blending tool. In keeping with this, W. Meier, J. Maslanik and C. Fowler have conducted an assimilation study using an Arctic ice model and 6 years of daily SSM/I displacements. They find that assimilation of SSM/I data yields motion fields with lower mean error and higher correlation relative to buoys than either the SSM/I or modeled motions alone. T. Agnew

has applied the individual motion fields to case studies of ice-atmosphere interactions. His work shows that combining motion vectors with imagery allows interpretation of features such as very large and extensive leads visible in the SSM/I gridded TBs. Other such case studies point out potential discrepancies in the modeled sea level pressure fields.

It is important to note that no single processing method and data-combination approach is likely to be best for all applications of the ice motion data. For example, some users may prefer a highly-filtered data set while other users will wish to use a data set with as little post processing applied as possible. An example of this contrast is the requirements of motion fields for model evaluation versus fields for data assimilation. For the former use, a heavily-processed data set consisting of blended vectors in the form of climatologies or monthly means may be most useful. However, for assimilation, the minimum amount of filtering, averaging, and merging with other data types is typically desirable. Even in the case of modeling, some users may wish to employ gridded motion fields with filtering based on winds or other ancillary information, while other users may wish to use motion data unmodified by such information.

Planned launch of the AMSR sensor, with spatial resolution for each channel roughly double that of SSM/I and with lower-frequency channels with resolution comparable to SSM/I's 37 GHz data, will offer the potential for substantially improved data sets. The improved resolution should yield displacements with standard deviations of perhaps 2 to 3 cm/s compared to buoys. Based on the SSM/I results, it appears likely that a single-channel, enhanced-resolution passive microwave sensor such as has been discussed as an experimental satellite could offer accuracies to within 1 cm/s for most of the year.